WHITEPAPER

MODELING OF SPT-100 STATIONARY PLASMA THRUSTER (HALL EFFECT THRUSTER)

(Published June 4, 2020)

Overview

Stationary plasma thrusters (SPT) [1,2] also known as Hall thrusters are among the most mature electric propulsion devices used in various space applications including satellite orbit correction and station keeping. Hall thruster uses large local electric field in plasma by using a transverse magnetic field to reduce electron conductivity. This electric field can extract positive ion from plasma and can accelerate them to high velocity in comparison with conventional chemical thrusters providing thrust. In spite of decades of research and development, due to involvement of nonlinear complex underlying physics, SPT phenomena is not fully understood. Rapid improvements in computational capability now allow numerical simulations that provide useful insight into such problems. To predict the performance of SPT as well to get more insights into SPT physics, a fast, robust, and accurate predictive simulation tool for Hall thruster plasma phenomena has been developed with the *VizGlow*™ plasma modeling framework. [3] The approach is based on hybrid plasma modeling approach with coupled Particle and Fluid models for different aspects of the physical phenomena. SPT-100 has been modeled by *VizGlow*™ software and benchmarked for experimental results of SPT-100.

Objective

The objective of the present study is to demonstrate the ability of simulating Hall thruster magnetic field configuration, gas flow, and non-equilibrium plasma modeling capability in *VizGlow*™.

Introduction

The key sub-physics that occurs in an SPT-100 are schematically illustrated in Figure 1. Propellant gas (xenon) is fed through a gas injector (inlet) that also serves as the anode for the HET discharge. The gas is ionized as it traverses the axial length of the thruster. The exhaust of the Hall thruster is mostly ions, i.e. the input feed gas is nearly fully ionized. The electrons for the thruster originate from a hollow cathode located outside the Hall thruster device that then streams towards the anode in the Hall thruster. A shaped magnetic field generated by an external electromagnet is used to magnetize the electrons as they stream from the cathode to the anode. The magnetized electrons transport is retarded in cross magnetic-field direction providing a measure of confinement for the electrons thus increasing their residence time and the effectiveness to ionize the feed gas.

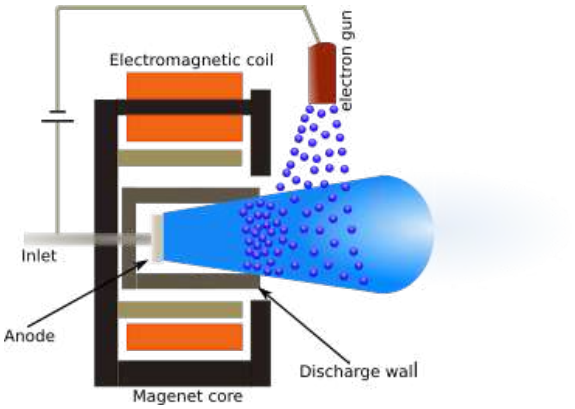

Figure 1: Schematic of Hall Effect Thruster.

Mathematical Formulation and Governing Equations

The plasma in the Hall thruster is described using a hybrid model of *VizGlow*™ simulation package. Hybrid model is based on technique that is reported in the literature. [4–7] In this model, all heavy species (neutrals, and ions) is solved using particle approach and the electrons are solved using fluid approach. The hybrid model is used to take advantage of strongly magnetized electrons so that the governing equation for electrons is needed only to resolve in the perpendicular direction to the magnetic field lines. Essentially all of the ingredients necessary for modeling and simulation of all kind of Hall thrusters are currently available in *VizGlow*™. Important physics associated with a Hall thruster operation include 1)magnetostatics fields, 2) gas flow physics in a rarefied environment, 3) excitation and ionization processes of a neutral gas in an imposed electric field, 4) magnetized plasma physics, 5) ion acceleration in electric field, and 6) plasma-wall interactions.

Magnetostatics Model

Magnetic field required to confine electrons in the Hall thruster are typically generated by coil currents and permanent magnetics (although coil currents are most common). The mathematical model predicts the magnetic induction ($\vec{B}$) in the Hall thruster geometry. The magnetic induction is defined in terms of term of the magnetic field strength ($\vec{H}$), the permanent magnetization ($\vec{M}$), and the permeability (μ) using the constitutive relation

$$\vec{B} = \mu\left(\vec{H} + \vec{M}\right) \tag{0.1}$$

Further defining in terms of a magnetic field vector potential ($\vec{A}$) such than

$$\vec{B} = \vec{\nabla} \times \vec{A} \tag{0.2}$$

The governing equation solved in the model domain is given by the Maxwell's equation as

$$-\nabla^2\vec{A} = \mu\vec{j}_{\text{ext}} + \mu\vec{\nabla} \times \vec{M} \tag{0.3}$$

where $\vec{j}_{\text{ext}}$ is the current density in the domain (here the coil currents). The first term on the right-hand side describes the generation of the magnetic field due to coil currents and the second term described the generation due to permanent magnetics (if there are any). The magnetostatics model is solved by the *VizEM* module within the Overviz Simulation framework.

Particle Model

A particle kinetic model is used in representing the neutral gas and charged particle kinetics. The two main features of the particle model are representation of the motion of the particles in the domain and their collisions amongst themselves and with boundaries of the domain, e.g. wall and non-wall open boundaries. The collisions can be complex; in the gas phase collisions can lead to simple momentum transfer among the participating particles, or can lead to changes in the identity of the particles, i.e. chemical reactions such as excitation and ionization. In our particle model we classify particles according to the chemical species. Each species is represented by a concept of a "simulated particle" meaning a representative particle that in fact describes a large number of real particles as defined by a particle weight (W_k). This particle weight is therefore defined as the ratio ,

$$W_k = \frac{N_{\text{real},k}}{N_{\text{sim},k}} \tag{0.4}$$

where $N_{\text{real},k}$ is the number of real particles of a particular species identified by index k and $N_{\text{sim},k}$ is the corresponding number of computationally simulated particles. The motion of each simulated particle is given by the classical Newton's law of motion as,

$$m_k\frac{d\vec{v}}{dt} = \vec{F} \tag{0.5}$$

where, m_k is the mass of the particle, $\vec{v}$ is the particle velocity, $\vec{F}$ is the force acting on the particle, and t is time. In the presence of electromagnetic field the charged particles experience a Lorentz force

$$\vec{F} = q\left(\vec{E} + \vec{c} \times \vec{B}\right) \tag{0.6}$$

where, q is the charge on the particle and $\vec{E}$ is the electric field. For neutral particles the charge is zero and the force acting on the particle is also zero. Finally, particles collide among themselves in "gas collisions" and will boundaries "wall collisions". The gas phase collisions are treated using the Monte-Carlo Collision (MCC) model. For each projectile species the probability of collision in a given time interval Δt is determined as

$$P_{\text{coll}} = 1 - exp\left(-n_{\text{targ}}g_{\text{pt}}\sigma_{\text{pt},r}\Delta t\right) \tag{0.7}$$

where n_{targ} is the number density of the target species, g_{pt} is the relative speed between the projectile and target species and $\sigma_{\text{pt},r}$ is the cross section of the specific reaction that involved the projectile and target species. The above particle modeling approach is implemented in the *VizGrain* particle module that is coupled with *VizGlow*™.

Table 1: Important dimensions in the SPT-100 geometry

Radial distance of channel centerline	42.5 mm
Channel length (channel entry to channel exit)	25 mm
Channel height	35 mm
Channel exit height	50 mm
Gas domain outside axial length	100 mm

Work Flow of Hybrid Model for Plasma Phenomena

The work flow of the hybrid model for Hall thruster simulations is shown in Figure 2. The hybrid model takes solution of the magnetic field (from the magnetostatics solver) as an input. Furthermore, it also takes the solution of a cold (neutral only, here Xe neutrals) gas flow through the thruster as initial conditions for the background flow solution. Although the neutral gas solution is updated during the plasma solve, an accurate cold gas initial flow is desirable for convergence of the plasma simulation. The cold gas flow is solved using the particle solver with only the Xe neutrals inflow into the domain subject to collisions.The hybrid plasma solver then solves for motion of Xe, Xe+, and Xe++ species using the particle solver and the electron temperature and electrostatic potential using the fluid approach. Quasineutrality is assumed to determine the electron density.

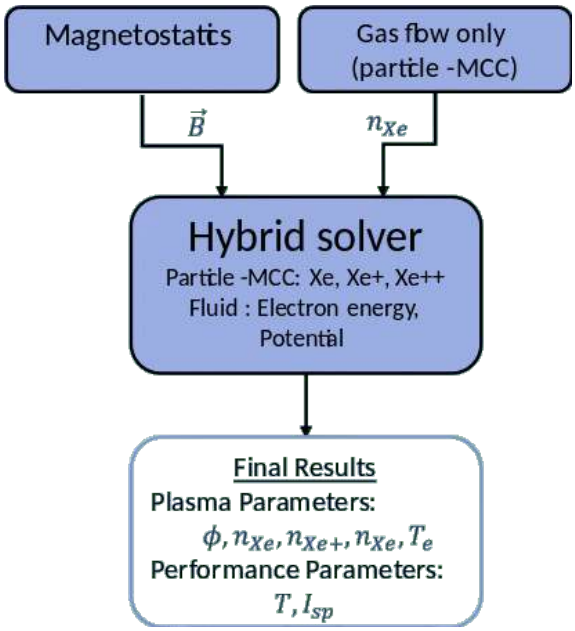

Figure 2: Work flow of the hybrid model for Hall thruster modeling.

Geometry of SPT-100 and Operating Parameters

The geometry for the Hall thruster is nominally axisymmetric and therefore the two-dimensional axisymmetric coordinate as indicated in the Figure 3 is used. All modeling performed here is 2D-axisymmetric. Some of the important geometric dimensions of the above thruster are shown in Table 1.

Computational mesh

The SPT-100 geometry is meshed using an unstructured mixed mesh with rectangles and triangular cells. Different meshes have been created for the simulations with different resolution and mesh type. This mesh comprises a total of over 17,000 cells with about 6067 in the gas domain where the plasma is solved for and a minimum mesh size of 1 mm. According to the mesh construction, the x-location of the anode face is at 0 mm, the center of channel is at 42.5 mm and the channel exit location is 25 mm.

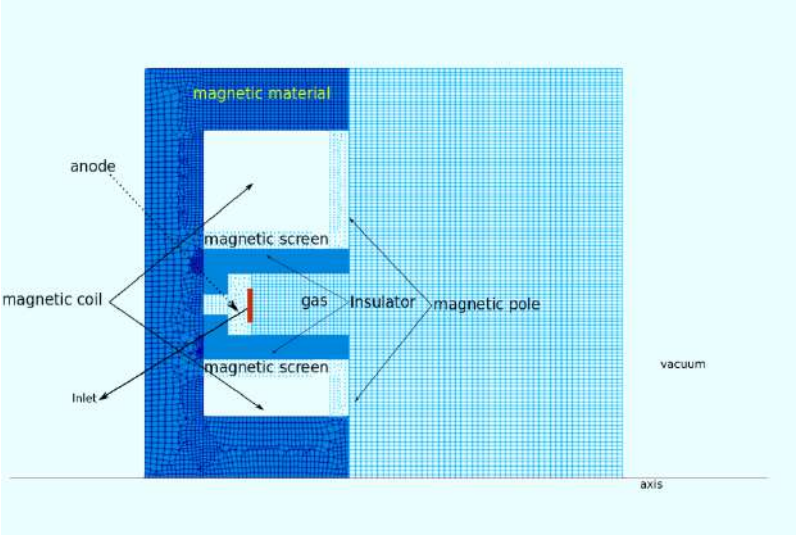

Figure 3: The geometry of the SPT-100 with of all major components including the gas channel, anode, magnetic circuit and coils for the generation of the magnetic field.

Table 2: Magnetic circuit parameters for baseline operation of SPT-100

Module	Description
Inner Coil # Turns	283
Inner Coil Current	2 A
Outer Coil # Turns	140
Outer Coil Current	2 A

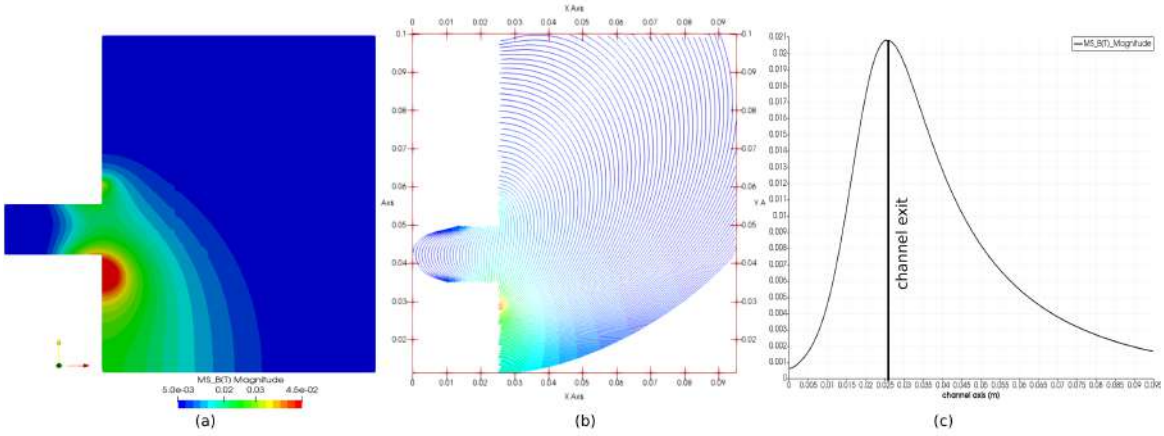

Figure 4: Results of magnetostatics simulations for the B-field in the (a) gas domain, (b) B-field streamlines in the gas domain, and (c) radial B-field at center of channel from anode to vacuum.

Results

Magnetostatics results

The first step in the modeling is to predict the magnetic fields in the computation domain. The entire geometry represented in Figure 3 is modeled for these simulations. In several literature articles, it is reported that the magnetic field in SPT-100 peaks at the exit channel and magnitude of field varies from 200-220 Gauss.[6] To obtain this magnetic field structure, the magnetic circuit parameters for the baseline conditions are given in Table 2. Results for the magnetic induction in the gas domain is shows in Figure 4. Figure 4(a) and 4(b) show results for the magnetic induction and magnetic field contour lines (magnetic streamlines) in plasma channel. The streamlines clearly show that the magnetic circuit is adequately designed to achieve good magnetic field topology by contouring of the lines to remain nearly parallel to walls, especially near the high B-fields at the channel exit. Figure 4(c) shows the magnetic field strength along the center line of channel axis. The radial B-field indicate the peak B-values peak just outside the channel exit. The B-field is found to peak at about 200 Gauss just outside the channel exit.

Xenon background gas flow

Table 3 presents the pure xenon background flow conditions for simulations. Total xenon mass flow rate 5 mg/s and the wall temperature is 700 K (all surfaces). The background gas flow in a SPT-100 typically has very low pressures (here $\sim$ 1 Pa) and as such cannot be represented using a continuum fluid model. We perform an initial simulation of the xenon gas flow to set the baseline flow in which the plasma is generated. The gas

Table 3: Xenon flow conditions for operation of SPT-100

Total xenon mass flow rate	5 mg/s
Wall temperature	700 K (all surfaces)

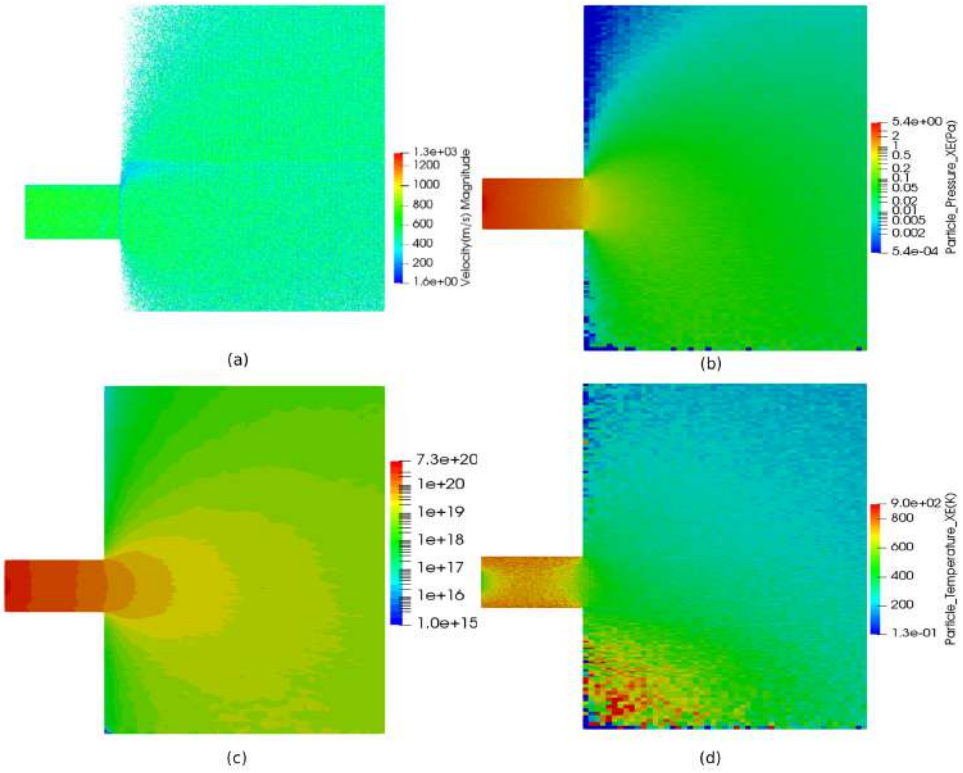

Figure 5: Results of Xenon gas flow at steady state,(a) particles colored by their velocity field (b) particle pressure (c) particle number density at log scale (d) particle temperature.

flow-only simulations are carried out using the particle method. Pure xenon gas enters the domain through inlets indicated in Figure 3 with 5 mg/s mass flow rate. Xenon gas enters through inlet with a temperature of 750 K and a number density of 6.187×10^{20} #/m^3. The particle simulation with xenon flow only run for a physical time of about 2 ms with a time-step of 10^{-6} s and it take a few hours of wall clock time on a single processor machine. Figure 5 shows results from the xenon flow only simulations. The gas enters the channel and is gradually accelerated out the channel into the vacuum. The number density of the gas is peaked at the inlets to a value of about 7.3×10^{20} #/m^3 corresponding to a pressure of ~3 Pa.

Plasma simulation results

The experimental parameters have been taken from Ref. 8 for SPT-100 operation and given in Table 4. The model parameters for simulations of SPT-100 have been mentioned in table 5. The magnetic streamlines are first constructed from the magnetic field solution. Figure 6 shows the magnetic streamlines (31 total) and the actual computation domain in which the electron energy and electrostatic potential are solved for. Figure 6 identifies the locations of the anode streamline and the cathode streamlines at which the anode and cathode conditions are actually imposed in the simulation. Table 6 shows the schematic of the plasma boundary conditions and boundary specification for the particles. The baseline simulation is run for a total of 150 microseconds of

Table 4: Experimental parameters for operation of SPT-100

Electrical circuit parameters:	
Anode potential (ϕ anode)	300 V
Cathode flow rate	1 mg/s
Xenon gas mass flow rate	5 mg/s
pressure facility	0.00018 Pa

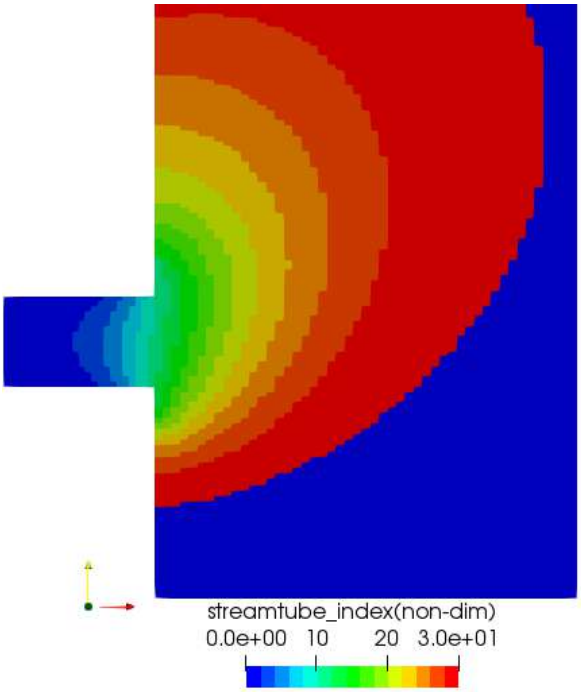

Figure 6: Streamline index and the actual computation domain in which the electron energy and electrostatic potential equations are solved.

physical time and is found to be adequate for converged solution. The particle statistical weights are 1×10^{11} for Xe neutrals, and 5×10^{9} for the charged species (Xe+ and Xe++). A time step of 10^{-10} second is used for the integrating the electron energy and potential equations. The particle model uses a time step of 10^{-8} sec. As will be discussed below, no true steady state is possible for the SPT-100 phenomena and only period steady state with an oscillatory solution about a mean is possible. Figure 7 shows a snapshot of the key plasma parameters of electron temperature, electron density, xenon neutral density, and electrostatics potential in the domain. The electrostatic potential is nearly uniform at the anode potential of 300 V throughout the length of the channel and drops sharply at the channel exit to near ground value of 0 V. The electric field therefore peaks sharply at the channel exit, corresponding to the location of the peak B-fields. The reason for this is well know: it is caused by the sharp decrease in electron mobility at the channel exit where the B-field confinement is the highest. The electron density (and the ion densities) are high just upstream of the channel exit. Peak plasma density is about 5×10^{18} m^{-3} . The ions (and electrons) stream out the channel due to the high E-fields at the channel exit to form the propulsive beam. The electron temperature peak shown in Figure 7 is about 50 eV and is also confined to the channel exit location. It must however be emphasized that the averaged electron temperature is lower than 50 eV owing to the oscillatory nature of the solution. The neutral density shows significant changes from the pure neutral flow. The neutrals are nearly completely consumed by the plasma immediately downstream of

Table 5: Plasma model parameters for baseline operation of SPT-100.

Electrical circuit parameters:	
Anode potential (ϕ_{anode})	300 V
Cathode potential (ϕ_{cathode})	0 V
Electron energy equation boundary conditions:	
Anode electron temp. ($T_{e,\text{anode}}$)	50,000 K
Cathode electron temp. ($T_{e,\text{cathode}}$)	20,000 K
Electron mobility model:	
Wall collision freq. factor (α)	0.1
Bohm mobility enhancement factor (α_{B} anode)	0.05 V
Electron energy wall loss model:	
Wall energy loss multiplier(α_ϵ)	0.01
Wall energy loss threshold energy (U)	20 eV
1D Domain:	
Number of streamlines	30

the channel exit results in a hole in the neutral density profile. We also note that we do not see any significant population of the Xe++ ion in the domain in our simulations in Figure 8. The reason for the same is not entirely clear since other reports have shown a small Xe++ population in the SPT-100 plume. Figure 9 shows transient profiles of the total current and the ion currents through the discharge. The currents are found to increase sharply during the initial phase of the discharge transient and eventually settle to a periodic steady state on a time scale of 100's microseconds. The oscillatory nature of the currents underscores the inherently oscillatory nature of the discharge. The average total current at steady state is about 4.75 A and the average ion current is about 5 A which is very well match with experimental result reported in Ref. 8. Finally, we discuss thruster performance metrics. Table 7 shows some metrics to characterize the ion beam. The thrust T calculated as the total momentum carried by the ions at the exit plane is calculated to be about 86.9 mN. Based on these values the specific impulse of the thruster $I_{sp} = \frac{T}{\cdot mg}$ can be calculated as about 1673 sec.

Table 8 presents some additional metrics for the thruster along with comparisons with experimental results. As indicated earlier, the total discharge current is about 5 A, the ion beam current is about 4.75 A. The discharge power $P_{\text{disch}} = I_t\,(\phi_{\text{anode}} - \phi_{\text{cathode}})$ is calculated to be about 1.425 kW where I_t is ion beam current. The ion beam power $P_{\text{ionbeam}} = \int\int \frac{1}{2} m_i^{\cdot} u_i^2 dS$ Integrated over the exit plane is calculated as about 3.02 kW. Hence the overall electrical efficiency of the thruster is $\eta_{\text{ion}} = \frac{P_{\text{ionbeam}}}{P_{\text{disch}}}$ is calculated at about 47.2 %.

Table 6: The particle model boundary condition specifications

Surface	Boundary Conditions
Inflow	Species: Xe inflow, Xe+ and Xe++ quenched
Anode Wall	Species: Xe+ and Xe++ quenched, Xe thermalized
Ceramic Wall	Species: Xe+ and Xe++ quenched, Xe thermalized
Inner/Outer Pole Wall	Species: Xe+ and Xe++ quenched, Xe thermalized
Outflow	Species: Species: All species exit domain

Table 7: Ion beam matrices from modeling results for thruster

Species	Flux F_k (#/s)	Thrust T_k (mN)	Beam Power (kW)
Xe+	1.71×10^{19}	66	–
Xe++	4.46×10^{18}	16	–
Xe	–	10^{-6}	–
Total	–	82 mN	$P_{\text{beam}} = 0.672$ kW

Table 8: Overall electrical performance comparison of modelling results and experimental results for thruster

Thruster Performance	VizGlow Model	Experimental
Discharge current	4.75	4.5
Power	1.425 kW	1.35 kW
Thrust	8N mN	86.9 mN
Specific impulse	1673	1470

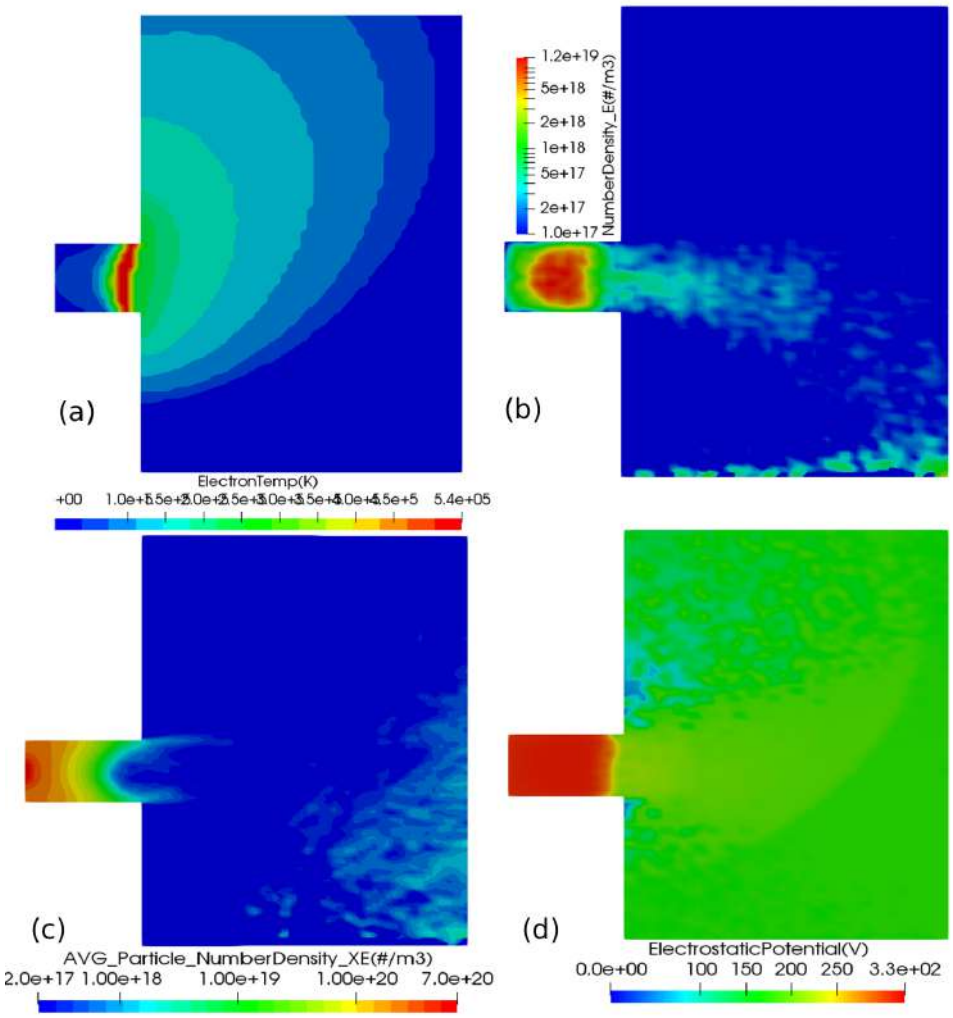

Figure 7: Results of plasma simulation at steady state,(a)Electron temperature, (b)Electron density, (c)Average neutral density of xenon, (d)Electrostatic potential 150 microseconds after the start of the simulation.

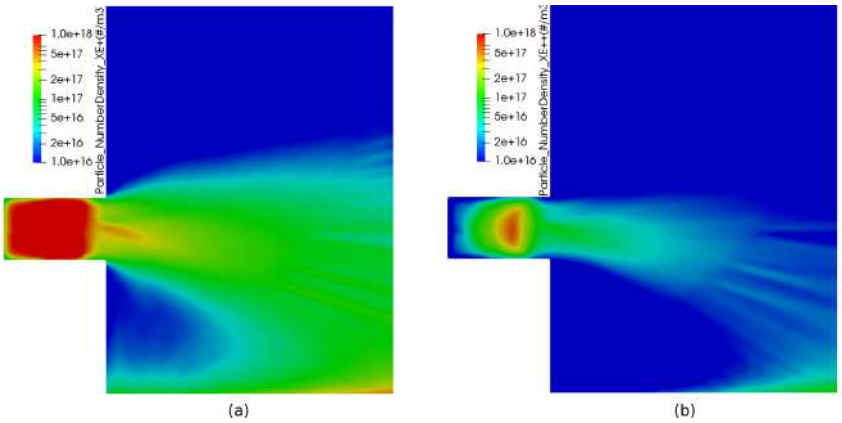

Figure 8: Xe+ (singly ionized xenon) and Xe++(doubly ionized xenon) density at 150 ms.

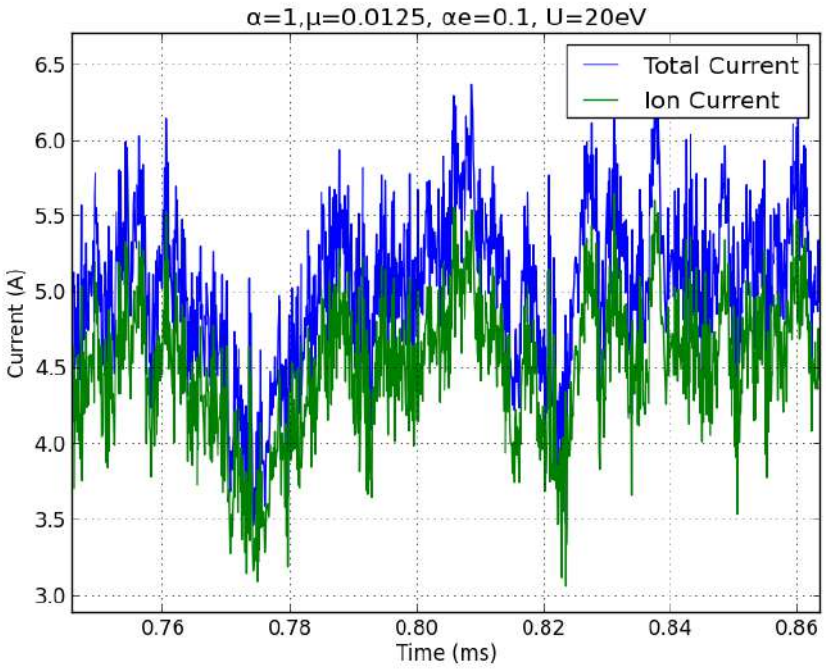

Figure 9: Total current and ion current in the discharge as a function of physical time simulated

References

[1] A. I. Morozov and V. V. Savelyev, *Fundamentals of Stationary Plasma Thruster Theory*, pp. 203–391. Boston, MA: Springer US, 2000.

[2] D. M. Goebel and I. Katz, *Fundamentals of Electric Propulsion: Ion and Hall Thrusters*. Wiley, 2008.

[3] EsgeeTeam.

[4] J. M. Fife, *Hybrid-PIC modeling and electrostatic probe survey of Hall thrusters*. Thesis (Ph.D.)–Massachusetts Institute of Technology, Dept. of Aeronautics and Astronautics, February 1999, 1998.

[5] R. R. Hofer, I. Katz, I. G. Mikellides, and M. G. Castano, "Heavy particle velocity and electron mobility modeling in hybrid-pic hall thruster simulations," *American Institute for Aeronautics and Astronautics*, p. 4658, 2006.

[6] G. J. M. Hagelaar, J. Bareilles, L. Garrigues, and J. P. Boeuf, "Two-dimensional model of a stationary plasma thruster," *Journal of Applied Physics*, vol. 91, p. 5592, 2002.

[7] J. W. Koo and I. D. Boyd, "Computational model of a hall thruster," *Computer Physics Communications*, vol. 164, no. 1, pp. 442 – 447, 2004. Proceedings of the 18th International Conferene on the Numerical Simulation of Plasmas.

[8] S. J. M., H. J. A., and H. T. W. pp. IEPC–93–094, 1993.

For additional information contact us,
or please visit **esgeetech.com**

ESGEE TECHNOLOGIES INC.
1301 S Capital of Texas Hwy., Suite B-330
Austin, Texas, 78746, USA